DEUTSCHES ELEKTRONEN – SYNCHROTRON

DESY 92-142
October 1992

Hard Scattering in γp Interactions

H1 Collaboration

ISSN 0418-9833

NOTKESTRASSE 85 · D-2000 HAMBURG 52

To be sure that your preprints are promptly included in the
HIGH ENERGY PHYSICS INDEX,
send them to (if possible by air mail):

DESY
Bibliothek
Notkestraße 85
W-2000 Hamburg 52
Germany

DESY-IfH
Bibliothek
Platanenallee 6
O-1615 Zeuthen
Germany

ISSN 0418-9833

DESY 92-142
20.10. 1992

Hard scattering in γp interactions

H1 Collaboration

T. Ahmed[3], V. Andreev[22], B. Andrieu[25], M. Arpagaus[32], A. Babayev[21], H. Bärwolff[31], J. Ban[15], P. Baranov[22], E. Barrelet[26], W. Bartel[11], U. Bassler[26], G.A. Beck[17], H.P. Beck[33], H.-J.Behrend[11], A. Belousov[22], Ch. Berger[1], H. Bergstein[1], G. Bernardi[26], R. Bernet[32], G. Bertrand-Coremans[4], M. Besancon[9], P. Biddulph[20], E. Binder[11], J.C. Bizot[24], V. Blobel[13], K. Borras[8], P.C. Bosetti[2], V. Boudry[25], C. Bourdarios[24], F. Brasse[11], U. Braun[2], W. Braunschweig[1], V. Brisson[24], D. Bruncko[15], J. Bürger[11], F.W. Büsser[13], A. Buniatian[11], S. Burke[17], G. Buschhorn[23], A.J. Campbell[10], T. Carli[25], F. Charles[26], D. Clarke[5], A.B. Clegg[16], M. Colombo[8], J.A. Coughlan[5], A. Courau[24], C. Coutures[9], G. Cozzika[9], L. Criegee[11], J. Cvach[25], J.B. Dainton[17], M. Danilov[21], A.W.E. Dann[20], W.D. Dau[14], M. David[9], E. Deffur[11], B. Delcourt[24], L. DelBuono[26], M. Devel[24], A. DeRoeck[11], P. Dingus[25], C. Dollfus[33], J.D. Dowell[3], H B. Dreis[2], A. Drescher[8], J. Duboc[26], D. Düllmann[13], O. Dünger[13], H. Duhm[12], M. Eberle[12], J. Ebert[30], T.R. Ebert[17], G. Eckerlin[11], V. Efremenko[21], S. Egli[33], S. Eichenberger[33], R. Eichler[32], F. Eisele[11], E. Eisenhandler[18] N.N. Ellis[3], R.J. Ellison[20], E. Elsen[11], M. Erdmann[11], E. Evrard[4], L. Favart[4], A. Fedotov[21], D. Feeken[13], R. Felst[11], J. Feltesse[9], Y. Feng[26], I.F. Fensome[3], J. Ferencei[11], F. Ferrarotto[29], W. Flauger[11,†], M. Fleischer[11], G. Flügge[2], A. Fomenko[22], B. Fomynich[21], M. Forbush[7], J. Formanek[28], J.M. Foster[20], G. Franke[11], E. Fretwurst[12], P. Fuhrmann[1], E. Gabathuler[17], K. Gamerdinger[23], J. Garvey[3], J. Gayler[11], A. Gellrich[13], M. Gennis[11], U. Gensch[31], H. Genzel[1], R. Gerhards[11], D. Gillespie[17], L. Godfrey[7], U. Goerlach[11], L. Goerlich[6], M. Goldberg[26], A.M. Goodall[17], I. Gorelov[21], P. Goritchev[21], C. Grab[32], H. Grässler[2], R. Grässler[2], T. Greenshaw[17], H. Greif[23], G. Grindhammer[23], C. Gruber[14], J. Haack[31], M. Haguenauer[25], D. Haidt[11], L. Hajduk[6], O. Hamon[26], D. Handschuh[11], E.M. Hanlon[16], M. Hapke[11], J. Harjes[13], P. Hartz[8], R. Haydar[24], W.J. Haynes[5], J. Heatherington[18], V. Hedberg[19], R. Hedgecock[5], G. Heinzelmann[13], R.C.W. Henderson[16], H. Henschel[31], R. Herma[1], I. Herynek[27], W. Hildesheim[26], P. Hill[11], C.D. Hilton[20], J. Hladky[27], K.C. Hoeger[20], Ph. Huet[4], H. Hufnagel[8], N. Huot[26], M. Ibbotson[20], M.A. Jabiol[9], A. Jacholkowska[24], C. Jacobsson[19], M. Jaffre[24], L. Jönsson[19], K. Johannsen[13], D. Johnson[4], L. Johnson[16], H. Jung[2], P.I.P. Kalmus[18] S. Kasarian[11], R. Kaschowitz[2], P. Kasselmann[12], U. Kathage[14], H. H.Kaufmann[31], I.R. Kenyon[3], S. Kermiche[24], C. Kiesling[23], M. Klein[31], C. Kleinwort[13], G. Knies[11], T. Köhler[1], H. Kolanoski[8], F. Kole[7], S.D. Kolya[20], V. Korbel[11], M. Korn[8], P. Kostka[31], S.K. Kotelnikov[22], W. Krasny[8,15], H. Krehbiel[11], D. Krücker[2], U. Krüger[11], J.P. Kubenka[23], H. Küster[11], M. Kuhlen[23], T. Kurca[15], J. Kurzhöfer[8], B. Kuznik[30], R. Lander[7], M.P.J. Landon[18] R. Langkau[12], P. Lanius[23], J.F. Laporte[9], A. Lebedev[22], U. Lenhardt[8], A. Leuschner[11], C. Leverenz[11], D. Levin[11], S. Levonian[22], Ch. Ley[2], G. Lindström[12], P. Loch[11], H. Lohmander[19], G.C. Lopez[18], D. Lüers[23,†], N. Magnussen[30], E. Malinovski[22], S. Mani[7], P. Marage[4], J. Marks[10], R. Marshall[20], J. Martens[30], R. Martin[17], H.-U. Martyn[1], J. Martyniak[6], S. Masson[2], A. Mavroidis[18] S.J. Maxfield[17], S.J. McMahon[17], A. Mehta[20], K. Meier[11], T. Merz[11], C.A. Meyer[33], H. Meyer[30], J. Meyer[11], S. Mikocki[15,24], V. Milone[29], E. Monnier[26], F. Moreau[25], J. Moreels[4], J.V. Morris[5], J.M. Morton[17], K. Müller[33], P. Murin[15], S.A. Murray[20], V. Nagovizin[21], B. Naroska[13], Th. Naumann[31], D. Newton[16], H. Nguyen[26], F. Niebergall[13], R. Nisius[1], G. Nowak[6], G.W. Noyes[3], M. Nyberg[19], H. Oberlack[23], U. Obrock[8], J.E. Olsson[11], S. Orenstein[25], F. Ould-Saada[13], C. Pascaud[24], G.D. Patel[17], E. Peppel[11], S. Peters[23], H.T. Phillips[3], J.P. Phillips[20], Ch. Pichler[12], W. Pilgram[2], D. Pitzl[32], R. Prosi[11], F. Raupach[1], K. Rauschnabel[8], P. Reimer[27], P. Ribarics[23], V. Riech[12], J. Riedlberger[32], M. Rietz[2], S.M. Robertson[3], P. Robmann[33], R. Roosen[4], A. Rostovtsev[21], C .Royon[9], M. Rudowicz[23], M. Ruffer[12], S. Rusakov[22], K. Rybicki[6], E. Ryseck[31], J. Sacton[4], N. Sahlmann[2], E. Sanchez[23], D.P. Sankey[5], M. Savitsky[11], P. Schacht[23], P. Schleper[1], W. von Schlippe[18], C. Schmidt[11], D. Schmidt[30] W. Schmitz[2], V. Schröder[11], M. Schulz[11], A. Schwind[31], V. Scobel[12], U. Seehausen[13], R. Sell[11], M. Seman[15], A. Semenov[21], V. Shekelyan[21], I. Sheviakov[22], H. Shooshtari[29], G. Siegmon[14], U. Siewert[14], Y. Sirois[25], I.O. Skillicorn[10], P. Smirnov[22], J. Smith[7], L. Smolik[11], Y. Soloviev[22], H. Spitzer[13], P. Staroba[27], M. Steenbock[13], P. Steffen[11], R. Steinberg[2], H. Steiner[26], B. Stella[29], K. Stephens[20], J. Strachota[11], U. Straumann[33], W. Struczinski[2], J.P. Sutton[20], R.E. Taylor[34,24], G. Thompson[18] R.J.Thompson[20], I. Tichomirov[21], C. Trenkel[14], P. Truöl[33], V. Tchernyshov[21], J. Turnau[6], J. Tutas[1], L. Urban[23], A. Usik[22], S. Valkar[28], A. Valkarova[28], C. Vallee[26], P. VanEsch[4], A. Vartapetian[11], J. Vasdik[22], M. Vecko[27], P. Verrecchia[9], R. Vick[13], G .Villet[9], E. Vogel[1], K. Wacker[8], I.W. Walker[16], A. Walther[8], G. Weber[13], D. Wegener[8], A. Wegner[11], H. P.Wellisch[23], S. Willard[7], M. Winde[31], G.-G. Winter[11], M.Th. Wolff[32], L.A. Womersley[17], A.E. Wright[20], N. Wulff[11], T.P. Yiou[26], J. Zacek[24,28], P. Zavada[27], C. Zeitnitz[12], H. Ziaeepour[24], M. Zimmer[11], W. Zimmermann[11], and F. Zomer[24]

[1] *I. Physikalisches Institut der RWTH, Aachen , Germany*
[2] *III. Physikalisches Institut der RWTH, Aachen , Germany*
[3] *School of Physics and Space Research, University of Birmingham, Birmingham, UK*
[4] *Inter-University Institute for High Energies ULB-VUB, Brussels, Belgium*
[5] *Rutherford Appleton Laboratory, Chilton, Didcot, UK*
[6] *Institute for Nuclear Physics, Cracow, Poland*
[7] *Physics Department and IIRPA, University of California, Davis, California, USA*
[8] *Institut für Physik, Universität Dortmund, Dortmund, Germany*
[9] *DAPNIA, Centre d'Etudes de Saclay, Gif-sur-Yvettes, France*
[10] *Department of Physics and Astronomy, University of Glasgow, Glasgow, UK*
[11] *DESY, Hamburg, Germany*
[12] *I. Institut für Experimentalphysik, Universität Hamburg, Hamburg, Germany*
[13] *II. Institut für Experimentalphysik, Universität Hamburg, Hamburg, Germany*
[14] *Institut f. Reine und Angewandte Kernphysik, Universität Kiel , Germany*
[15] *Institute of Experimental Physics, Slovak Academy of Sciences, Kosice , CSFR*
[16] *School of Physics and Materials, University of Lancaster, Lancaster, UK*
[17] *Department of Physics, University of Liverpool, Liverpool, UK*
[18] *Queen Mary and Westfield College, London, UK*

[19] *Physics Depa[redacted]t, University Lund , Lund, Sweden*
[20] *Physics Depar[redacted]nt, University of Manchester, Manchester, UK*
[21] *Institute for Theoretical and Experimental Physics, Moscow, Russia*
[22] *Lebedev Physical Institute, Moscow, Russia*
[23] *Max-Planck-Institut für Physik, München, Germany*
[24] *LAL, Universite de Paris-Sud, Orsay, France*
[25] *LPNHE, Ecole Polytechnique, IN2P3-CNRS, Palaiseau, France*
[26] *Universites Paris VI and VII, LPNHE, Paris, France*
[27] *Institute of Physics, Czechoslovak Academy of Sciences, Praha, CSFR*
[28] *Nuclear Center, Charles University, Praha, CSFR*
[29] *INFN Roma and Dipartimento di Fisica, Universita "La Sapienzia", Roma, Italy*
[30] *Fachbereich Physik, Bergische Universität Gesamthochschule Wuppertal, Wuppertal, Germany*
[31] *DESY, Institut für Hochenergiephysik, Zeuthen, Germany*
[32] *Institut für Mittelenergiephysik, ETH, Zürich, Switzerland*
[33] *Physik-Institut der Universität Zürich, Zürich, Switzerland*
[34] *Stanford Linear Accelerator Center, Stanford Californa, USA*
† *Deceased*

Abstract

We report on the investigation of the final state in interactions of quasi-real photons with protons. The data were taken with the H1 detector at the HERA *ep* collider. Evidence for hard interactions is seen in both single particle spectra and jet formation. The data can best be described by inclusion of resolved photon processes as predicted by QCD.

1 Introduction

The study of hard scattering reactions in photoproduction is an area of considerable theoretical and experimental interest. It allows the investigation of the interaction of *real* photons with quarks and gluons inside the nucleons. Until now experiments were limited by the center of mass (CM) energy achievable with existing photon beams.

The recently commissioned electron-proton storage ring HERA at the DESY laboratory in Hamburg, Germany, collides electrons of 26.7 GeV with protons of 820 GeV beam energy. Utilizing the quasi-real photons exchanged between electrons and protons at very small electron scattering angles opens a new energy domain for the study of γp interactions.

The data analysed in this paper were collected during the first data-taking period of the H1 detector at the HERA collider in June-July 1992. Preliminary results have already been presented in ref.[1], a similar investigation is described in [2]. The runs selected for the present analysis correspond to an integrated luminosity of 883 $\mu b^{-1}\pm$ 10%.

2 Detector description and event selection

In this paper we describe in outline the main components of the H1 collider detector and refer to [3] for details.

Charged particles from the interaction region are measured in two cylindrical tracking detectors (central and forward [1]) which together are 4 m long and 1.7 m in diameter. The chambers are surrounded by a fine grained liquid argon calorimeter with a geometry optimized for the very different beam energies of the two colliding particles. The calorimeter consists of an electromagnetic section with a thickness varying between 20 and 30 radiation lengths, and a hadronic section with a thickness between 4 and 8 interaction lengths. It covers polar angles between 4° and 155°. The energy resolutions are for electrons $\sigma(E)/E = 0.12/\sqrt{E}$ and for hadrons $\sigma(E)/E = 0.5/\sqrt{E}$ with E in GeV. The backward region ($154° < \Theta < 176°$) is covered by a proportional chamber followed by a lead-scintillator calorimeter (BEMC) with approximately the same energy resolution for electrons as that of the liquid argon calorimeter. All these detectors are inside an octagonal iron yoke with a total length of 9.6 m and height of 8.7 m. This provides a thickness of ~ 4 interaction lengths and is instrumented with streamer tubes to detect muons and the tail of the hadronic energy. A superconducting coil provides a homogeneous axial field of 1.2 Tesla in the tracking volume. Muon detection is supplemented by a forward muon spectrometer with a toroidal magnet covering the region $5° < \Theta < 20°$.

A luminosity detector measuring the reaction $e + p \rightarrow e + \gamma + p$ is placed in the backward direction with components at $z = -33$ m to tag small angle electrons and at $z = -100$ m to measure photons. Each component consists of a crystal calorimeter with an energy resolution of $\sigma(E)/E = 0.1/\sqrt{E}$.

We consider two different data samples in this analysis, tagged electron events and events with large transverse energy E_T.

2.1 Tagged electron events

Events with electrons in the small angle tagger, $e + p \rightarrow e + hadron + X$, were recorded to study single particle distributions. The hardware trigger for this event sample was a coincidence between an electron in the electron tagger system and at least one 'ray' signal from the central tracking detector. The electron trigger was derived from the crystal calorimeter which accepts electrons with scattering angles below 5 mrad with the energy threshold set to 4 GeV. The single ray trigger for hadrons in the central tracker was based on two double layers of cylindrical proportional chambers with radii $R \approx 16$ cm and $R \approx 52$ cm. Their cathode pads provide space points which are used to form rays in sectors of the azimuthal angle φ and the projection of the ray in the $R - z$ plane. At least three out of four pad layers in a sector were required to fire the trigger.

Offline the single ray requirement was sharpened by demanding at least one track in the central tracker satisfying the following conditions: a) more than 10 hits out of maximal 56, b) first reconstructed point on the track less than 30 cm from the beam axis, c) distance of closest approach (DCA) to the beam axis less than 2 cm, d) distance along the beam axis from the nominal interaction point at DCA at most 50 cm, e) polar angle in the range $30° < \Theta < 150°$, and f) a transverse momentum p_T of more than 0.3 GeV. This requirement on tracks suppressed background from beam wall interactions.

[1] We call the direction of the unscattered proton 'forward', coinciding with the polar angle $\Theta = 0°$ and the positive z-coordinate. 'Backward' refers to the electron direction.

The remaining background contribution is dominated by random coincidences between electrons hitting the electron tagger and proton-gas events in the H1 interaction region.

Candidates for ep scattering events were found by a selection based on the scaled photon energy $y = p \cdot q / p \cdot k$ calculated using firstly the tagged electron and secondly the final state hadrons. The four-vectors describe the incoming proton p, the incoming electron k and the photon q. Using the tagged electron y is well approximated by $y_e = 1 - E'/E$, where E, E' denote the incoming and the scattered electron energies. For the final state hadrons y can be expressed by the sum of energies and momenta along the z axis $y_h = \Sigma_i (E^{(i)} - p_L^{(i)})/2E$ [4]. The variable y_h was calculated using the cell energies of the liquid argon and of the BEMC calorimeters.

For background studies a proton-gas sample was recorded using a proton pilot bunch[2]. In this sample most of the energy is found in the forward direction causing y_h to be concentrated below 0.2. Background from accidental coincidences between tagged electrons and proton-gas scattering was therefore suppressed by demanding $y_h > 0.2$. Background from electron-gas events was eliminated by requiring an energy deposition $E_{fwd} \geq 5$ GeV within a 25° cone around the forward direction.

A region of good acceptance in the electron tagger system was selected by demanding $0.35 < y_e < 0.7$. The lower cut in y_e was optimized for a minimum background contribution using the shape of the electron energy spectrum from electron pilot bunch data (fig. 1a, dashed histogram). This background sample was scaled to have the same number of events as the ep sample above the maximum accepted electron energy. With the pessimistic assumption that all events from the ep sample above this cut were background events an upper limit of 9% was derived for the contamination of the ep sample due to beam-gas events. The final sample after these cuts consists of 330 tagged electron events.

Several methods were employed to confirm the purity of the tagged electron sample. In the event sample from the proton pilot bunch the final state charge distribution measured with tracks from the central track detector was found to have a positive charge excess. Neither the tagged electron sample nor the γp Monte Carlo show this effect. Further tests have been based on a) the number of protons identified using the ionization in the central jet chamber, b) the position of the event vertex along the beam axis (fig. 1b) and c) the shape of the rapidity distribution of charged tracks. These studies confirm that the final sample contains predominantly events from ep scattering.

2.2 Large E_T events

A second event sample was used to study inclusive jet production, $e + p \rightarrow e + jet + X$. The final state electron is either measured in the electron tagger or escapes unseen in the very backward direction.

The hardware trigger consisted of a z-vertex trigger [5]: a 1-dimensional histogram was filled online with the intercepts of rays along the beam axis and a peak search was

[2]The name pilot bunch refers to proton (electron) bunches without an electron (proton) bunch partner in the interaction region.

performed. If the peak height was significantly above the expectation from background the event was accepted.

A candidate sample for high p_T- jets was selected offline by requiring a transverse energy (E_T) of at least 10 GeV in the H1 calorimeter ($\Theta > 25°$). In contrast to the single particle spectra discussed above the limited statistics excludes the use of an electron tagging criterion as a main signature for ep interactions. A potential source of background is due to halo muons and hadrons accompanying the proton beam. They can be removed by comparing the energy measured in the calorimeter and in the tracker and requiring that $E_{tracker}/E_{calo} > 0.2$ in the range $25° < \Theta < 150°$. A veto on muon candidates in the H1 instrumented iron suppresses the background from cosmic rays that have survived the previous cuts. A cut on electron candidates with $E > 10$ GeV in the backward region ($140° < \Theta < 176°$) eliminates events from deep inelastic scattering reactions. Finally electron beampipe and proton beampipe events were removed from this sample by requiring the tracks to originate from the interaction region in the transverse plane. The data sample treated in this way should contain only high E_T events due to photoproduction from almost real photons along with events from beam-gas interactions.

In the next step we applied a jet classification cone algorithm with a cone size of $\Delta R = \sqrt{\Delta\eta^2 + \Delta\varphi^2} < 1.0$, where the symbols η and φ denote the pseudorapidity and the azimuthal angle of the calorimeter clusters. The cone algorithm follows the 'Snowmass accord' [6] but with an increased cone radius because of the much lower energy of the jet candidates. The minimum transverse energy contained inside the cone had to be 3 GeV.

Monte Carlo simulations of high E_T photoproduction[3] predict a rather flat distribution of the opening angle between the two highest E_T cones. The data show such a distribution, however with an additional peak at small opening angles which was found to be dominated by proton-gas interactions. A 60° cut on the opening angle drastically reduces this background.

The data sample with an opening angle $< 60°$ between the two cones can be further used for a quantitative estimate of the remaining beam-gas background. This is done by utilizing the fact that the vertex distributions measured along the z-axis looks very different for both these samples. A z-vertex cut of $|z| < 40$ cm was applied. From the ratio of events outside to those inside this cut in the sample with beam-gas candidates a contamination of 7% in our ep sample was estimated.

A visual scan of the 51 events remaining after these cuts, together with other quantitative checks (charge distribution, number of protons) show that this sample is of similar quality to that discussed above for the single particle spectra. In fact our sample contains 10 events with a tagged outgoing electron.

Besides the event sample just described we have 9 further events which are triggered by the electron tagger system, but not by the z-vertex trigger, and survived all other cuts described. The global z-vertex trigger efficiency of 53% derived from the tagged events agrees well with Monte Carlo simulations of the trigger.

[3]The parameters of the simulation are explained in section 3.

3 Rapidity and transverse momentum distributions of charged particles

The pseudorapidity, η, distribution of charged particles in hadronic reactions has been measured in many previous experiments and found to have a rectangular distribution with rounded edges. It is centered around the rapidity of the center of mass system and the width of the distribution depends on the logarithm of the CM energy W.

In the tagged electron event sample the energy of the γp system reaches values in the range $175 < W < 250$ GeV. The rapidity of the γp system as measured in the H1 laboratory frame is in the forward direction at $\eta_{\gamma p} \approx 2$. The high CM energy should give rise to a rapidity plateau of width ± 5 units extending well beyond the region covered by the central tracking detector. Fig. 2a shows the observed track distribution for $|\eta| < 1.3$.

Figure 2b shows the distribution of the squared transverse momentum, p_T^2, of these particles. For $p_T^2 < 1$ GeV the steeply falling distribution is consistent with a Gaussian distribution of particles with a width of $\sigma_{p_T} \approx 0.35$ GeV. Above $p_T^2 > 1$ GeV we observe a second component: a tail of high transverse momentum particles, indicating hard scattering processes.

For comparison with theory the generator RAYVDM [7] is used for the 'soft' processes which are simulated according to the vector dominance model. For the 'hard' processes the PYTHIA [8] generator is used which includes direct (γ gluon fusion and QCD Compton scattering) and 'resolved' photon interactions with the partons of the incoming protons. In the latter processes the partonic content of the photon, as defined by the photon structure function ('resolved' photon) participates in the hard scattering reaction with partons inside the proton. Note that the photon structure function contains a hadronic piece which accounts for hard scattering reactions already expected in the vector dominance model. The PYTHIA simulation used the Drees-Grassie[9] parametrization of the photon structure function and the M-T B1 proton structure function[10]. The cut on the minimum transverse momentum $\hat{p}_{T,min}$ of the hard process was varied, the other parameters remaining at their default values. Initial and final state parton showers are taken into account, and the fragmentation of partons to hadrons follows the Lund scheme [11]. The H1 detector response was simulated with a detailed program based on the GEANT package [12], and the simulated events were then reconstructed with the same reconstruction program as used for the data.

Figure 2 compares predictions of these Monte Carlo simulations with the measured data. The dashed line represents the result of the 'soft' processes only. The full line shows the 'soft' plus QCD prediction (PYTHIA, $\hat{p}_{T,min} = 2.5$ GeV). The shape of the rapidity distribution is well described by both models. In the case of the squared transverse momentum the shape at low p_T^2 is also well described by both models, however the tail at high transverse momenta, which is expected to result from hard scattering processes, is only reproduced by the PYTHIA Monte Carlo.

4 Jets in direct and resolved photon processes

It is well known[13] that in the p_T range investigated here, QCD predicts a dominance of the resolved photon processes leading to a (3+1)-jet final state [4]. Although initially the spectator partons in the photon have small p_T this is not necessarily the case for the resulting jet due to parton showering and fragmentation processes. We therefore do not expect the final state to exhibit a distinct two jet structure reproducing the hard scattering of partons at the Born level.

With these caveats in mind the kinematical properties of the two highest E_T cones of our final sample were compared to predictions from the PYTHIA generator (see section 3.1). In all quantities studied (E_T balance, correlation in azimuthal angle, energy flow in transverse plane, transverse sphericity) we found agreement with the simulation. From this agreement we identify the jets defined by our cones with the hadrons produced by parton fragmentation. The average rapidity η of the jets is 0.52 and the average observed center of mass energy $\sqrt{\hat{s}}$ in the hard scattering process is 12.5 GeV.

In tagged events the energy of the incoming photon is known and thus the momentum vectors of the two outgoing jets in direct processes are constrained. At the parton level without initial state radiation this constraint is given by

$$\frac{2E_\gamma}{E_T} = \tan\frac{\Theta_1}{2} + \tan\frac{\Theta_2}{2},$$

where Θ_1 and Θ_2 are the polar angles of the outgoing partons with equal transverse energy E_T. The result of a Monte Carlo simulation of jet production processes is shown in fig. 3a including resolved and direct processes and in fig. 3b for direct processes only. It can be seen that direct processes seldom lead to events where both jets have an angle Θ less than about 100°. For our luminosity we expect 0.6 events from direct processses in this region. This is in conflict with the data (fig. 3c), where 9 of the 19 tagged events are in the 'suppressed' region, suggesting that a large proportion of the observed events is not due to direct processes.

Supporting evidence for the dominance of resolved photons comes from inclusive jet rates. In fig. 4 the differential jet-p_T spectrum of jets in our 51 events is plotted. No attempt has been made to convert the measured transverse momentum of the cones to a true p_T. The absolute prediction of the PYTHIA generator is given by the solid line. The figure clearly demonstrates that for $p_T > 10$ GeV the shape of the data is well reproduced and that the absolute number of jets above this threshold agrees with the prediction roughly within a factor of 2. In comparing data with simulation it should be noted that besides the many assumptions used in the Monte Carlo calculation (e.g. choice of structure functions and scales) an error of 5% in the energy scale of the calorimeter at this stage of the calibration changes the predicted rate in the high p_T tail of the spectrum by a factor of 1.5.

We emphasize that the jet cross section in PYTHIA is calculated in the Born approximation and is thus highly divergent. A cut on the minimum transverse momentum ($\hat{p}_{T,min}$) of the generated partons has therefore always to be included. This minimum

[4] We use a jet counting scheme, where the '+1' indicates the additional jet from the proton remnant.

transverse momentum is 1 GeV for the solid line in fig. 4. The dashed dotted line is calculated for $\hat{p}_{T,min} = 5$ GeV. As would be expected both predictions agree for $p_T > 10$ GeV. At smaller p_T the distribution is sensitive to the uncertainties due to fragmentation and detector resolution. The absolute number of events predicted for both $\hat{p}_{T,min}$ cuts is 130 and 30 events respectively.

The dashed-dotted line in fig. 4 is the Monte Carlo prediction for the direct processes ($\hat{p}_{T,min} = 1$ GeV) only giving 7.3 events in total. It follows that the model which does not include the resolved photon contributions cannot explain the jet rate seen in our experiment.

The photon remnant jet produces hadrons predominantly in the very backward region, where only a small hadron flow from direct processes is expected. This can be seen in fig. 5 where the energy flow per event is plotted versus the polar angle Θ. A cut on the polar angle of the two highest E_T cones ($\Theta_{1,2} < 100°$) was applied. It separates the backward region i.e. the domain of the photon remnant by one unit in rapidity from these jets. The data (open points) are compared to the full Monte Carlo simulation with a $\hat{p}_{T,min}$ cut of 3 GeV (full line) and the simulation including direct processes only (dotted line). The energy flow in the backward region seen in the data is further evidence for the presence of the resolved photon processes.

5 Conclusions

In summary, we have studied interactions of quasi-real photons with protons in a new energy domain. We have seen clear evidence for hard interactions in single particle spectra and in jet production already with the first data available shortly after the startup of HERA. All quantities studied are in agreement with the predictions of QCD. We conclude from absolute jet rates, from angular correlations of the two highest p_T jets and from a study of the energy flow that resolved photon processes as required in QCD are present in the data.

Acknowledgements

We are very grateful to the HERA machine group whose outstanding efforts made this experiment possible. We acknowledge the support of the DESY computer center. We appreciate the many contributions of our engineers and technicians who constructed and mantained the detector. We thank the funding agencies for financial support of this experiment. The non-DESY members of the collaboration also want to thank the directorate for the hospitality extended to them.

References

[1] F. Eisele, Invited talk, Proceedings of the 26th International Conference on High Energy Physics, Dallas, 1992

[2] ZEUS collaboration, M. Derrick et al., DESY 92-138, submitted to Phys. Lett. B

[3] F. Brasse, Invited talk, Proceedings of the 26th International Conference on High Energy Physics, Dallas, 1992

[4] A. Blondel and F. Jacquet, Proceedings of the study of an ep facility for Europe, Ed. U. Amaldi, DESY 79/48 (1979) 391

[5] S. Eichenberger et al., Proc. 6th Int. Wire Chamber Conf., Vienna (1992), Nucl.Inst. and Methods, to be published

[6] J.E. Huth et al., Fermilab-Conf-90/249-E

[7] H1 interface program to LUCVDM of the LUCIFER package of G.Ingelman and A.Weigend (see DESY 87-018), Computer Phys. Comm. 46 (1987) 241

[8] T. Sjöstrand, PYTHIA at HERA, Proc. Workshop 'Physics at HERA', DESY, Hamburg (1991), Vol. 3 p. 1405 (eds.W. Buchmüller and G. Ingelman)

[9] M. Drees and G. Grassie, Z.Phys.C 28 (1985) 451

[10] J.G. Morfin and W.K. Tung, Z.Phys. C52 (1991) 13.

[11] T. Sjöstrand, Computer Phys. Comm. 39 (1986) 347, T. Sjöstrand and M. Bengtsson, Computer Phys. Comm. 43 (1987) 367

[12] GEANT program manual, CERN program library (1992)

[13] W. Stirling and Z. Kunszt, Proc. HERA Workshop, DESY, Hamburg (1987), Vol. 1, p. 331 (R.D. Peccei ed.)

Figure Captions

Fig.1: a) Energy spectrum of tagged electrons for ep data (full line). The arrows mark the range of the selected events. The dotted line indicates the spectrum of the background events. b) Vertex distribution along the beam axis for ep data.

Fig.2: a) Pseudorapidity and b) squared transverse momentum of charged tracks from ep data compared with a 'soft' (dashed line) and 'soft + QCD' Monte Carlo simulation (full line).

Fig.3: Correlation of the two highest p_T jets in polar angle for events with an electron tag. a) Monte Carlo prediction for resolved and direct processes, b) for direct processes only, c) correlation of the 19 e-tag events.

Fig.4: Inclusive p_T distribution of jets with $p_T > 3$ GeV. The solid line is the prediction of the PYTHIA program for $\hat{p}_{T,min} = 1$ GeV, the dashed dotted line corresponds to $\hat{p}_{T,min} = 5$ GeV. The dashed dotted line is the prediction if resolved photon contributions are excluded ($\hat{p}_{T,min} = 1$) GeV.

Fig.5: Histogram of energy flow per event versus polar angle Θ. The open points represent the data, the full line is taken from the Monte Carlo simulation for resolved and direct processes, whereas the dotted line gives the prediction for direct processes only.

Fig. 1

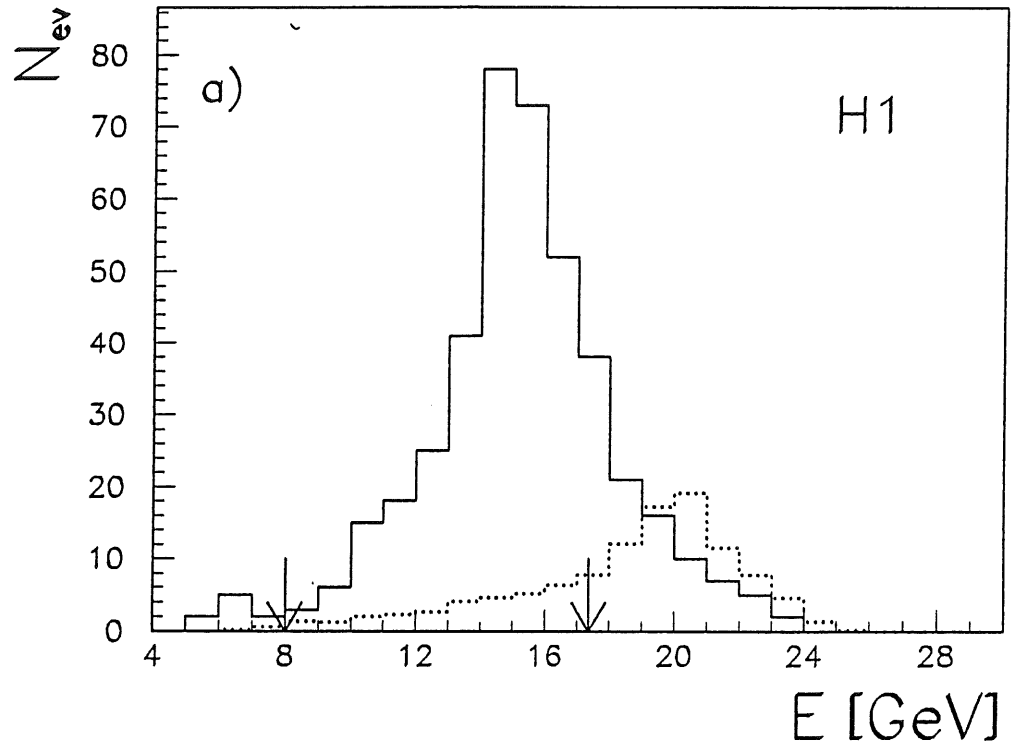
N_{ev}
a)
H1
0
10
20
30
40
50
60
70
80
4
8
12
16
20
24
28
E [GeV]

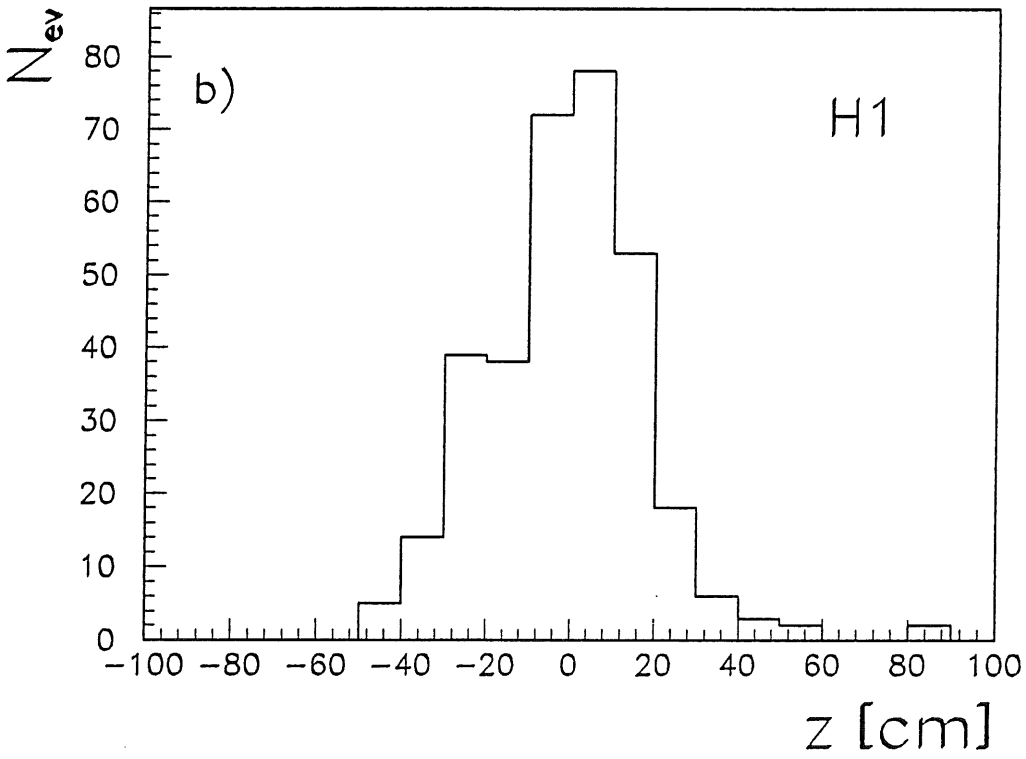
N_{ev}
b)
H1
0
10
20
30
40
50
60
70
80
−100
−80
−60
−40
−20
0
20
40
60
80
100
z [cm]

Fig. 2

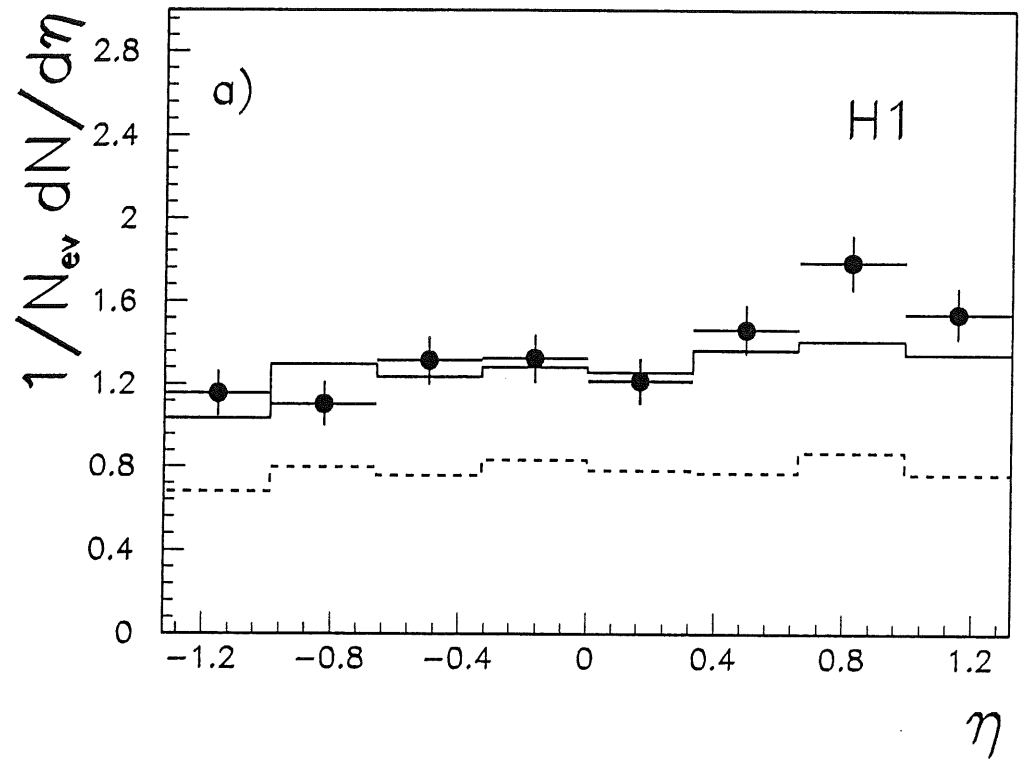
a)
H1
$1/N_{ev}\ dN/d\eta$
2.8
2.4
2
1.6
1.2
0.8
0.4
0
−1.2
−0.8
−0.4
0
0.4
0.8
1.2
η

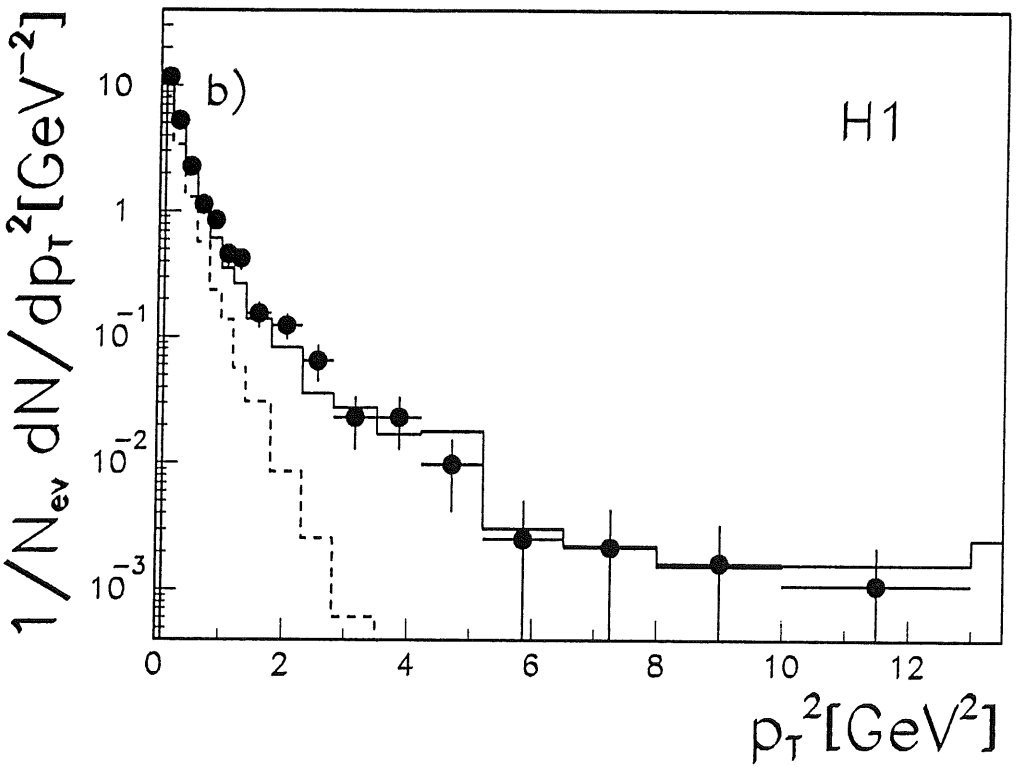
b)
H1
$1/N_{ev}\ dN/dp_T^2[GeV^{-2}]$
10
1
10^{-1}
10^{-2}
10^{-3}
0
2
4
6
8
10
12
$p_T^2[GeV^2]$

Fig.3

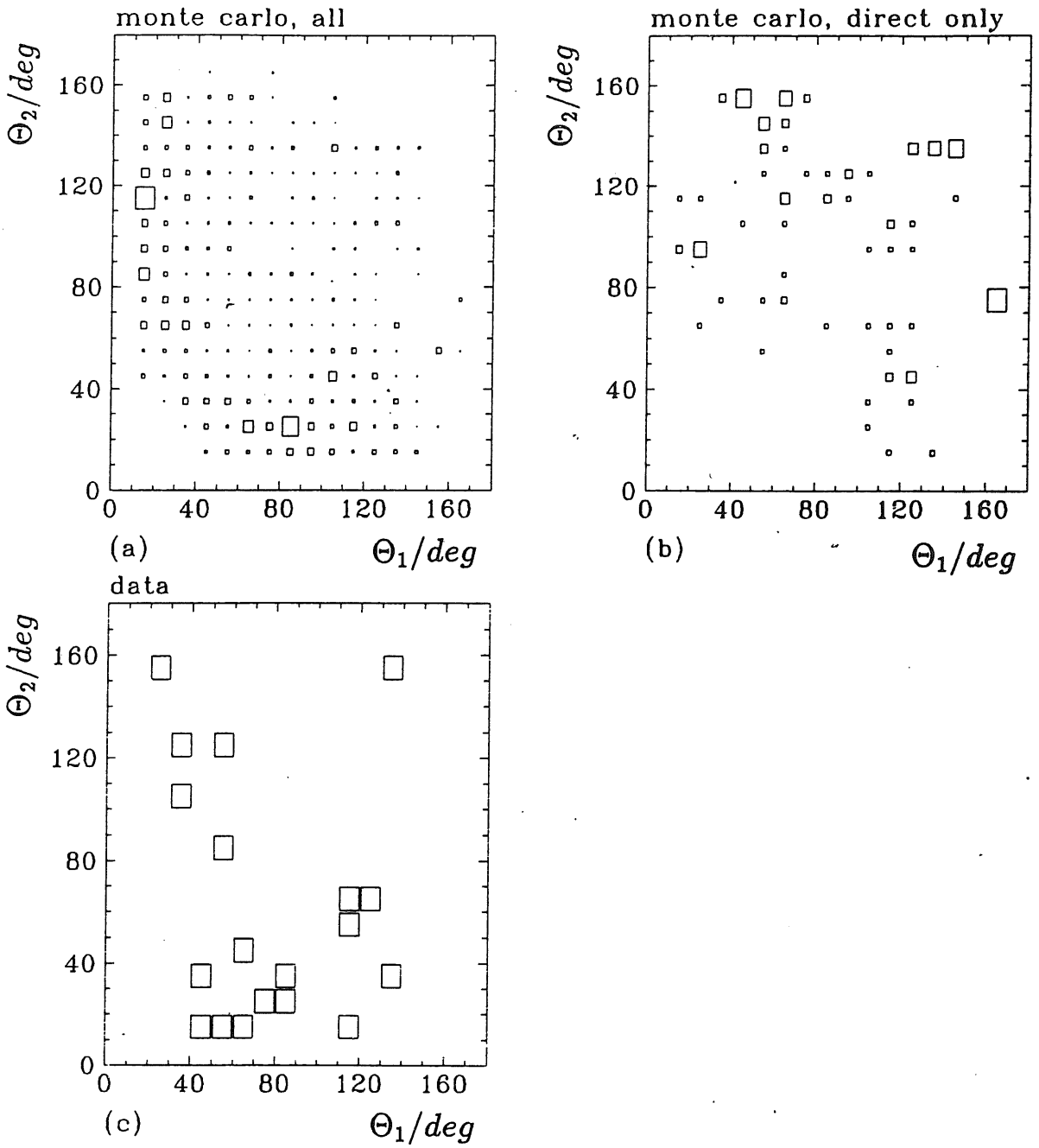
monte carlo, all
Θ_2/deg
160
120
80
40
0
0
40
80
120
160
(a)
Θ_1/deg
monte carlo, direct only
Θ_2/deg
160
120
80
40
0
0
40
80
120
160
(b)
Θ_1/deg
data
Θ_2/deg
160
120
80
40
0
0
40
80
120
160
(c)
Θ_1/deg

Fig.4

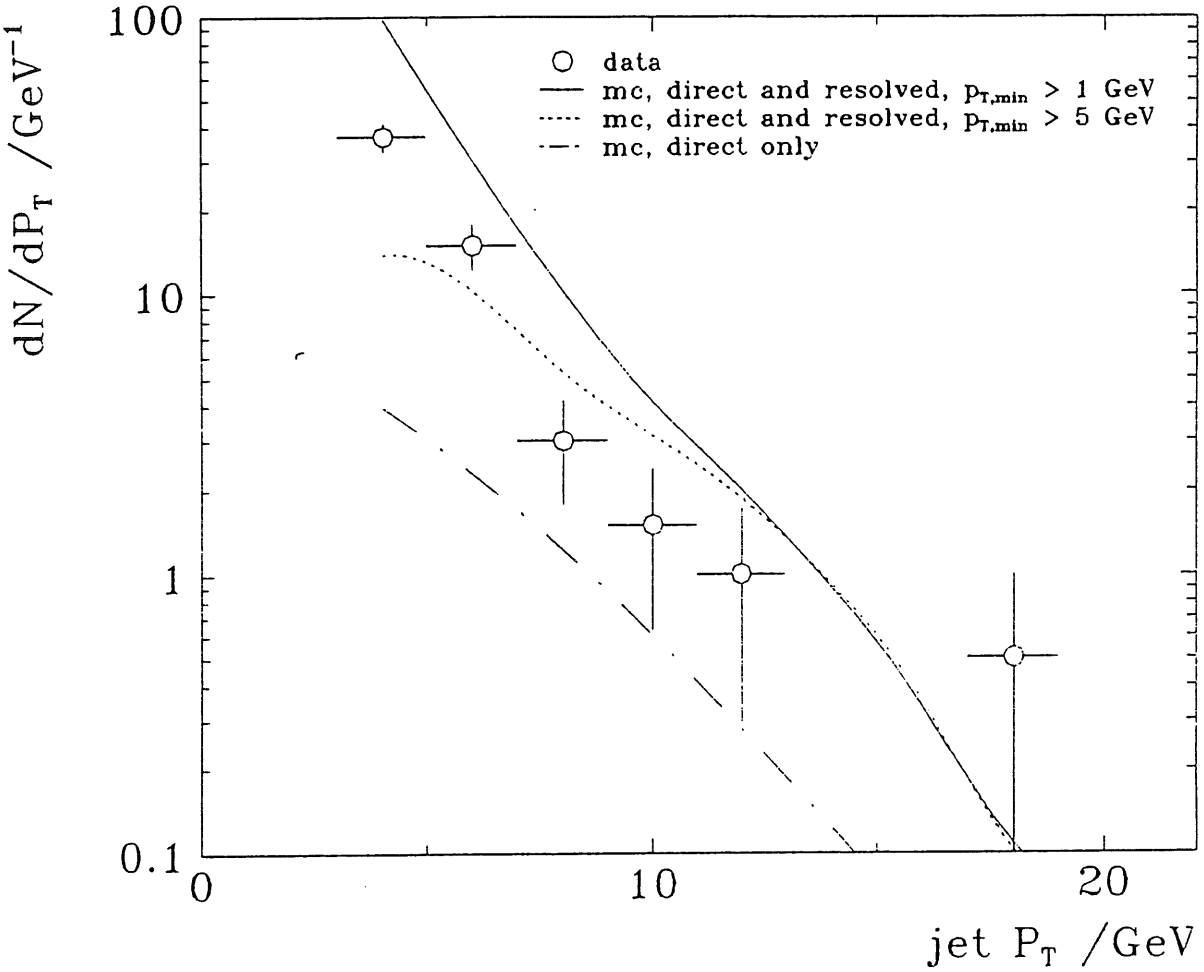
100
10
1
0.1
0
10
20
dN/dP$_T$ /GeV^{-1}
jet P$_T$ /GeV
data
mc, direct and resolved, p$_{T,min}$ > 1 GeV
mc, direct and resolved, p$_{T,min}$ > 5 GeV
mc, direct only

Fig.5

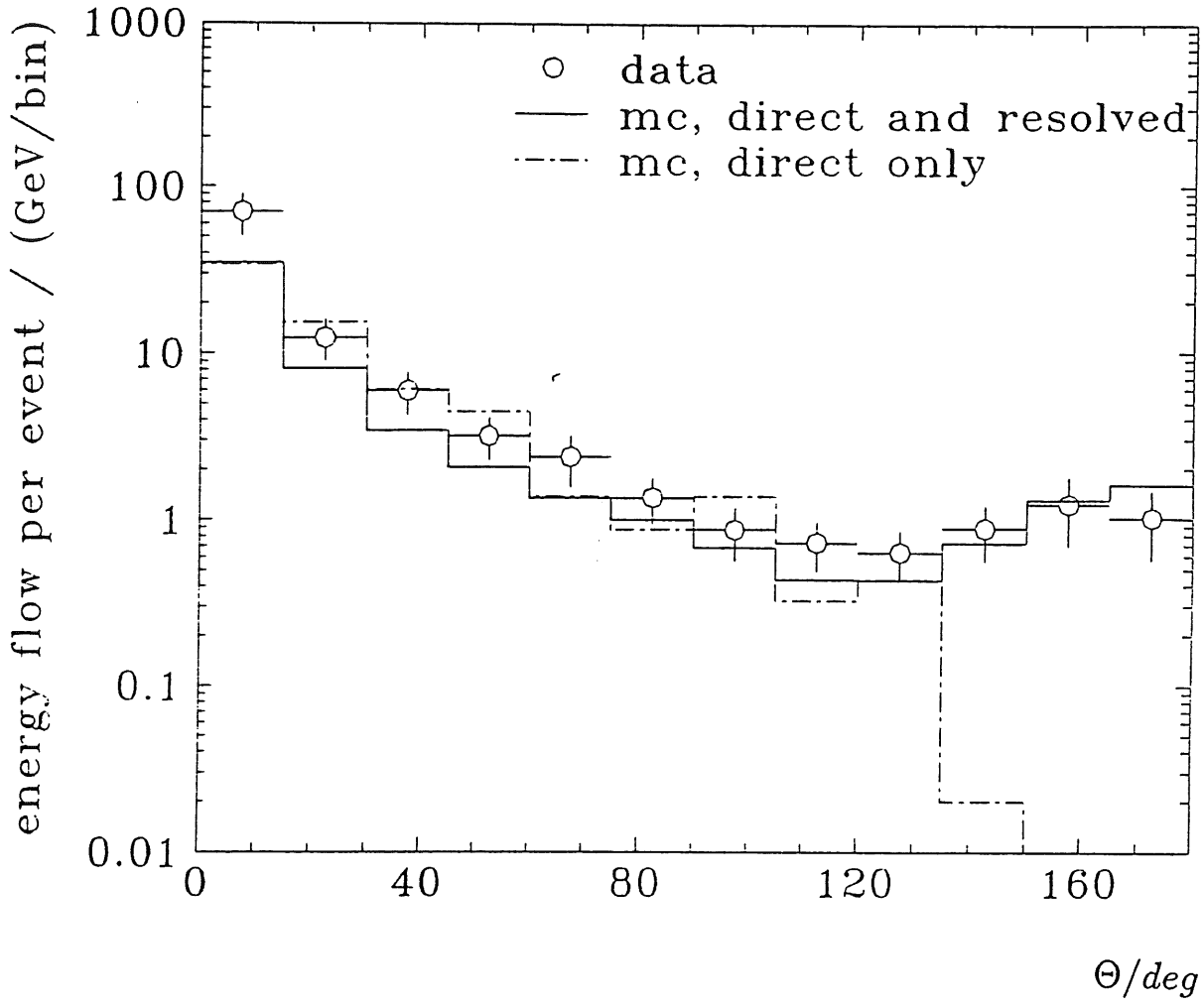
data
mc, direct and resolved
mc, direct only
energy flow per event / (GeV/bin)
1000
100
10
1
0.1
0.01
0
40
80
120
160
Θ/deg